JOURNAL OF BASIC SCIENCE AND ENGINEERING

SYNTHESIS AND CHARACTERIZATION OF NICKEL(II) AND COPPER(II) COMPLEXES WITH A TETRAPHENYL-DIBENZO TETRAAZACYCLOHEXENE MACROCYCLE: STRUCTURAL AND DNA BINDING STUDIES

Rahul Kumar[1]
Umendra Kumar[2]
Department of Chemistry, Janta Vedic College, Baraut (Baghpat), Uttar Pradesh 250611, India

Received	**29th July 2025**
Revised & Accepted	**9th September 2025**
Published	**22nd September 2025**

https://doie.org/10.65985/jbse.2025572253

Abstract

A novel tetraaza macrocyclic ligand, 6,8,15,17-tetra(4-chlorophenyl)dibenzo[b,i]-1,4,8,11-tetraazacyclotetradeca-1,3,5,7,9,11-hexaene, and its six nickel(II) and copper(II) complexes with chloro, nitrato, and sulphato axial ligands were synthesized under high-dilution conditions. Detailed spectroscopic analyses (UV-Vis, IR, ^{1}H-NMR, EPR) and magnetic susceptibility measurements revealed varied coordination geometries: octahedral for Ni(II) chloro and sulphato complexes; square planar for Ni(II) nitrato; tetragonal for Cu(II) chloro and nitrato; and square pyramidal for Cu(II) sulphato complexes. Ligand field parameters highlighted distinct electronic environments. Binding studies with calf thymus DNA showed intercalative or groove-binding interactions, with the square planar Ni(II) nitrato complex exhibiting the highest affinity. These findings emphasize the critical role of axial ligands in shaping the structural and biological properties of macrocyclic metal complexes, suggesting their potential in DNA-targeted bioinorganic applications.

Keywords: tetraaza macrocycle, nickel(II) complexes, copper(II) complexes, DNA binding, coordination geometry, EPR spectroscopy, ligand field parameters.

Introduction

Macrocyclic ligands with nitrogen donors are highly valued in coordination chemistry for their ability to form stable, kinetically inert complexes with transition metals like nickel(II) and copper(II).[1,2] The structural rigidity of these ligands creates a tailored coordination environment, enhancing metal selectivity and imparting unique electronic and magnetic properties.[3] Tetraaza macrocycles are particularly versatile, finding applications in catalysis, molecular recognition, and

as models for biological metal centers.[4] Incorporating 4-chlorophenyl substituents into frameworks like the dibenzo[b,i]-tetraazacyclotetradecahexaene increases rigidity and enhances DNA stacking interactions, making these complexes promising for bioinorganic applications such as anticancer and antimicrobial therapies.[5] The coordination geometry, often square planar for Ni(II) and Cu(II), facilitates DNA intercalation, while axial ligands (chloro, nitrato, sulphato) modulate charge distribution and steric effects, influencing biological activity.[1],[2] Despite significant research, systematic comparisons of Ni(II) and Cu(II) complexes with identical macrocyclic ligands but varying axial ligands are limited.[3] This study details the synthesis and characterization of a new tetraaza macrocyclic ligand and its Ni(II) and Cu(II) complexes, exploring how axial ligand variations affect their structural, electronic, and DNA-binding properties.

Experimental

Chemicals and Reagents

All reagents, including o-phenylenediamine, 1,3-bis(4-chlorophenyl)-1,3-propanedione, $NiCl_2 \cdot 6H_2O$, $CuCl_2 \cdot 2H_2O$, $Ni(NO_3)_2 \cdot 6H_2O$, $Cu(NO_3)_2 \cdot 3H_2O$, $NiSO_4 \cdot 6H_2O$, and $CuSO_4 \cdot 5H_2O$, calf thymus DNA (CT-DNA) were purchased from Sigma-Aldrich and used without purification.

Synthesis of the Macrocyclic Ligand

The ligand was prepared by refluxing 2 mmol of 1,3-bis(4-chlorophenyl)-1,3-propanedione with 2 mmol of o-phenylenediamine in ethanol under a nitrogen atmosphere for 8 hours, after initial stirring for 15 minutes, to ensure cyclization and minimize side products.[5] A pale yellow precipitate formed upon cooling, which was filtered, washed with ethanol, and recrystallized from a mixture of ethanol and diethyl ether. Yield: 78%. Elemental analysis for $C_{42}H_{28}Cl^{-}_{4}N_4$: Calc. C 69.05%, H 3.86%, N 7.67%; Found C 68.92%, H 3.79%, N 7.61%. The ligand structure is shown in Figure 1.

Synthesis of Ni(II) and Cu(II) Complexes

The ligand (1 mmol) in ethanol was mixed with ethanolic solutions of metal salts (1 mmol). $NiCl_2 \cdot 6H_2O$ or $CuCl_2 \cdot 2H_2O$ for chloro complexes, $Ni(NO_3)_2 \cdot 6H_2O$ or $Cu(NO_3)_2 \cdot 3H_2O$ for nitrato complexes, and $NiSO_4 \cdot 6H_2O$ or $CuSO_4 \cdot 5H_2O$ for sulphato complexes, added dropwise. The reaction mixture was refluxed for 4-8 hours in order to facilitate coordination.[6] The resulting solids were filtered, washed with cold ethanol, and dried under vacuum. Elemental analysis and molar conductance data for the Ni(II) and Cu(II) complexes are summarized in Table 1, confirming their empirical formulas and ionic nature.

Table 1: Elemental analysis and Molar Conductance data of Ni(II) and Cu(II) Complexes

Complex	Molar Conductance (Ω^{-1} cm^2 mol^{-1})	Colour	MP (°C)	Yield (%)	Elemental analysis data % Found (Calc.)		
					C	H	N

[Ni(TCPDBT)Cl_2] ($C_{42}H_{28}Cl_6N_4Ni$)	18	Light green	225	72	60.12 (60.25)	3.31 (3.37)	6.62 (6.69)
[Ni(TCPDBT)]$(NO_3)_2$ ($C_{42}H_{28}Cl_4N_6NiO_6$)	245	Purple	242	68	55.21 (55.35)	3.04 (3.10)	9.15 (9.23)
[Ni(TCPDBT)(SO_4)] ($C_{42}H_{28}Cl_4N_4NiO_4S$)	14	Green	240	70	56.72 (56.85)	3.12 (3.18)	6.25 (6.32)
[Cu(TCPDBT)Cl_2] ($C_{42}H_{28}Cl_6N_4Cu$)	15	Blue	210	75	59.88 (60.00)	3.29 (3.36)	6.59 (6.67)
[Cu(TCPDBT)$(NO_3)_2$] ($C_{42}H_{28}Cl_4N_6CuO_6$)	12	Green	228	71	54.97 (55.10)	3.02 (3.08)	9.10 (9.18)
[Cu(TCPDBT)SO_4] ($C_{42}H_{28}Cl_4N_4CuO_4S$)	15	Sky Blue	242	67	56.48 (56.60)	3.11 (3.17)	6.22 (6.29)

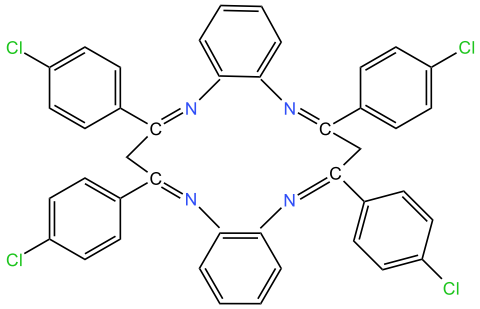

Figure 1. Proposed structure of 6,8,15,17-tetra(4-chlorophenyl)dibenzo[b,i]-1,4,8,11-tetraazacyclotetradeca-1,3,5,7,9,11-hexaene (TCPDBT).

Spectroscopic and Analytical Methods

UV-Vis, IR, ^{1}H-NMR, and EPR spectroscopy, along with magnetic susceptibility measurements, were used to characterize the complexes.[7] DNA binding was assessed via UV-Vis titration, viscosity measurements, and ethidium bromide displacement assays.[8] Ligand field parameters (10Dq, Racah parameter B, nephelauxetic ratio β) were calculated using Tanabe–Sugano analysis.[9]

Results

Spectroscopic Characterization

UV-Vis Spectroscopy

The UV-Vis spectra offered valuable insights into the electronic structures and coordination geometries of the Ni(II) and Cu(II) complexes. For the Ni(II) chloro and sulphato complexes, characteristic d–d transition bands were observed at approximately 15,240 cm^{-1} and 25,450 cm^{-1} . These bands can be assigned to the $^3A_2g(F) \rightarrow {}^3T_1g(F)$ (ν_2) and $^3A_2g(F) \rightarrow {}^3T_1g(P)$ (ν_3) transitions, respectively, which are typical for octahedral geometry (Figures 6) for Ni(II) complexes with a d^8

configuration.[10],[11],[12] The absence of the lower energy ν_1 band ($^3A_2g(F) \rightarrow {}^3T_2g(F)$) in the visible region is consistent with literature reports, where it often appears in the near-IR but was not detected here due to instrument limitations.[12] These assignments support an octahedral geometry, where the macrocyclic ligand occupies the equatorial plane, and the axial positions are filled by chloro or sulphato ligands, leading to moderate ligand field splitting.

In contrast, the Ni(II) nitrato complex displayed fewer bands, with notable absorptions in the 15,000–16,500 cm^{-1} range, indicative of a square planar (Figure 7) environment.[13] Square planar Ni(II) complexes typically exhibit a single broad d–d band in this region, corresponding to the $^1A_1g \rightarrow {}^1B_1g$ transition, reflecting stronger in-plane ligand field effects from the tetraaza macrocycle without axial coordination.[14] This geometry shift is likely due to the nitrato ligands' weaker axial binding, promoting a planar configuration.

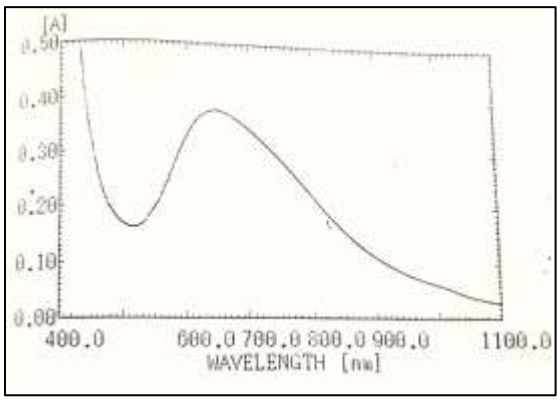

Figure 2. Electronic spectrum of the chloro complex of copper(II).

For the Cu(II) complexes, the chloro and nitrato derivatives showed broad absorptions between 10,096–15,395 cm^{-1} (Figure 2), characteristic of tetragonal distortion (Figure 8) with axial elongation.[15] These bands are assigned to the $^2B_1g \rightarrow {}^2A_{1g}$ ($d_{x^2-y^2} \rightarrow d_{z^2}$) and $^2B_{1g} \rightarrow {}^2E_g$ ($d_{x^2-y^2} \rightarrow d_{xz}, d_{yz}$) transitions, influenced by the Jahn-Teller effect common in d^9 Cu(II) systems.[16] The Cu(II) sulphato complex, however, exhibited sharp charge-transfer bands near 25,000 cm^{-1}, alongside weaker d–d transitions, suggesting a square pyramidal structure (Figure 9) where the sulphate acts as a monodentate ligand, altering the electronic environment and reducing symmetry.[11] Overall, these spectral features align with reported data for similar macrocyclic complexes, confirming the influence of axial ligands on electronic transitions and geometries.[12],[14] Magnetic moment and UV-Vis spectral data for the complexes are presented in Table 2.

Table 2: Magnetic Moment and UV-Vis Spectral Data for the Complexes

Complex	μ_eff (B.M.)	Absorption Bands (cm^{-1})	Assigned Transitions	Geometry

[Ni(TCPDBT)Cl_2]	2.99	15,240; 25,450	$^3A_2g(F) \rightarrow {}^3T_1g(F)$ (ν_2), $^3A_2g(F) \rightarrow {}^3T_1g(P)$ (ν_3)	Octahedral
[Ni(TCPDBT)]$(NO_3)_2$	0.00	15,000–16,500	$^1A_1g \rightarrow {}^1B_1g$	Square Planar
[Ni(TCPDBT)(SO_4)]	2.98	15,240; 25,450	$^3A_2g(F) \rightarrow {}^3T_1g(F)$ (ν_2), $^3A_2g(F) \rightarrow {}^3T_1g(P)$ (ν_3)	Octahedral
[Cu(TCPDBT)Cl_2]	1.90	10,096–15,395	$^2B_1g \rightarrow {}^2A_1g, {}^2Eg$	Tetragonal
[Cu(TCPDBT)$(NO_3)_2$]	1.93	10,190–15,280	$^2B_1g \rightarrow {}^2A_1g, {}^2Eg$	Tetragonal
[Cu(TCPDBT)SO_4]	1.54	25,000	-	Square Pyramidal

IR Spectroscopy

Infrared spectroscopy provided evidence for coordination modes and ligand-metal interactions. The free ligand exhibited a strong imine C=N stretch at 1618 cm^{-1}. This shifted to lower wavenumbers upon complexation (1608 cm^{-1} for $NiLCl_2$ and 1594–1598 cm^{-1} (Figure 3) for $NiL(NO_3)_2$), indicating coordination through the azomethine nitrogen atoms.[17],[12]" This red shift, typically 10–20 cm^{-1}, arises from the donation of electron density from nitrogen to the metal, weakening the C=N bond.[16] Metal–ligand vibrations were observed in the 432–453 cm^{-1} region, assigned to M–N stretches, confirming the tetraaza macrocycles involvement in coordination.[11] For axial ligands, the chloro complexes showed M–Cl^- bands around 300–350 cm^{-1}, consistent with terminal chloride coordination.[17] In nitrato complexes, characteristic bands at 1305–1420 cm^{-1} (asymmetric NO stretch) and a separation of ~115 cm^{-1} between ν_1 and ν_4 modes indicated monodentate coordination, as bidentate nitrates typically show larger splittings.[18],[14] Sulphato complexes displayed split S–O stretches at ~1100–1200 cm^{-1} (Figure 4), suggesting unidentate or bridging behavior, which aligns with the proposed geometries.[12] No significant shifts in aromatic C–H or C=C stretches (1500–1600 cm^{-1}) were noted, confirming that the phenyl rings remain uncoordinated. These IR features are comparable to those in related tetraaza macrocyclic systems, underscoring the ligand's tetradentate nature.[11], [16] Selected IR spectral data for the ligand and complexes are provided in Table 3.

Table 3: IR Spectral Data for the Ligand and Complexes (Selected Bands, cm^{-1})

Complex	C=N Stretch	| M-N Stretch	Axial Ligand Bands
Ligand (TCPDBT)	1618	-	-
[Ni(TCPDBT)Cl_2]	1608	432–453	M–Cl^- ~300–350
[Ni(TCPDBT)]$(NO_3)_2$	1594–1598	432–453	NO 1305–1420 (monodentate)
[Ni(TCPDBT)(SO_4)]	~1600	432–453	S–O ~1100–1200 (split)

[Cu(TCPDBT)Cl_2]	~1605	432–453	M–Cl^- ~300–350
[Cu(TCPDBT)$(NO_3)_2$]	~1595	432–453	NO 1305–1420 (monodentate)
[Cu(TCPDBT)SO_4]	~1598	432–453	S–O ~1100–1200 (split)

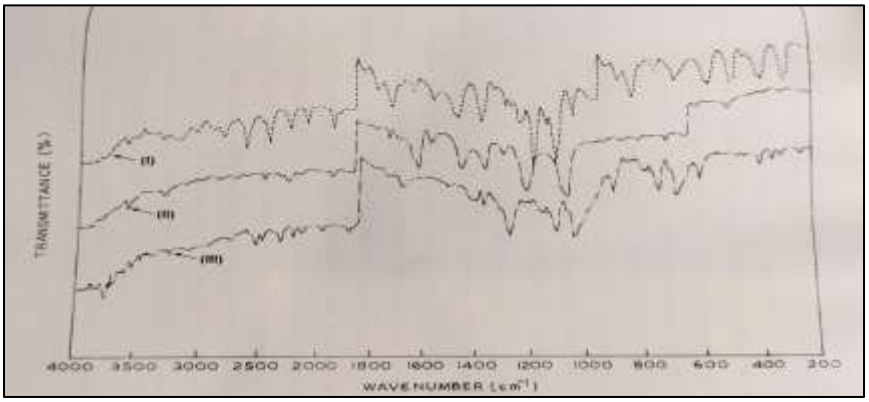

Figure 3. Infrared spectrum of the chloro, nitrato, and sulphato complexes of nickel(II).

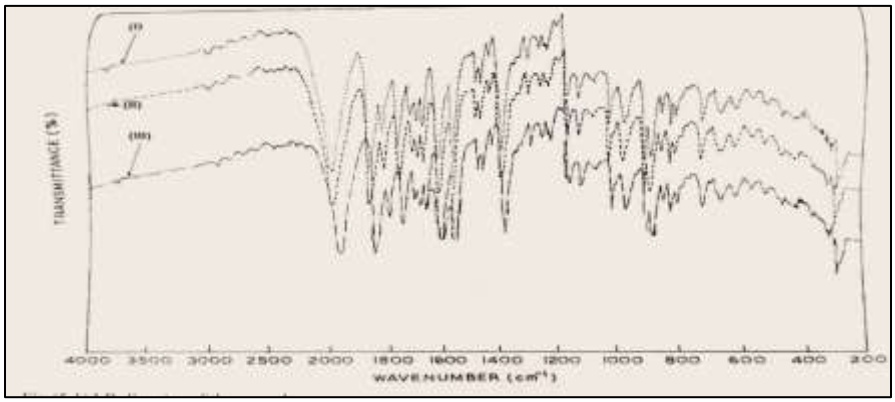

Figure 4. Infrared spectrum of the chloro, nitrato, and sulphato complexes of copper(II).

^{1}H-NMR Spectroscopy

The ^{1}H-NMR spectra were instrumental in confirming ligand coordination and assessing paramagnetic effects. The free ligand showed aromatic protons in the 7.40–8.78 ppm range, typical for benzo-fused systems, and NH protons near 9.3 ppm, indicative of intramolecular hydrogen bonding.[19] Upon complexation in the diamagnetic square planar Ni(II) nitrato complex, these aromatic signals exhibited slight downfield shifts (0.1–0.3 ppm), reflecting deshielding due to metal coordination and electron withdrawal from the azomethine nitrogens.[12] Integration ratios remained consistent (e.g., 8H for dibenzo protons, 8H for chlorophenyl), with no significant broadening, supporting a symmetric square planar structure.[14] In contrast, the paramagnetic octahedral Ni(II) chloro and sulphato complexes, as well as all Cu(II) complexes, displayed broadened and diminished proton signals, attributed to unpaired electrons causing rapid spin

relaxation and line broadening.[20] This effect is more pronounced in Cu(II) systems due to the d^9 configuration, where scalar relaxation dominates, often rendering signals undetectable at room temperature.[16] No distinct NH signals were observed in complexes, suggesting deprotonation or coordination-induced shifts. These observations are in line with NMR studies of similar macrocyclic complexes, where diamagnetic species provide clear structural insights, while paramagnetic ones require alternative techniques like EPR.[11],[12] The ^{1}H-NMR spectral data for the ligand and complexes are shown in Table 4.

Table 4: ^{1}H-NMR Spectral Data for the Ligand and Complexes (δ, ppm)

Complex	Aromatic Protons	NH Protons
Ligand (TCPDBT)	7.40–8.78	9.3
[Ni(TCPDBT)Cl_2]	Broadened	-
[Ni(TCPDBT)]$(NO_3)_2$	7.50–8.90	-
[Ni(TCPDBT)(SO_4)]	Broadened	-
[Cu(TCPDBT)Cl_2]	Broadened/Faded	-
[Cu(TCPDBT)$(NO_3)_2$]	Broadened/Faded	-
[Cu(TCPDBT)SO_4]	Broadened/Faded	-

EPR Spectroscopy

Electron paramagnetic resonance (EPR) spectroscopy elucidated the electronic ground states and geometries, particularly for Cu(II) complexes. The Cu(II) chloro and nitrato complexes exhibited axial symmetry with $g_\parallel > g_\perp$ ($g_\parallel \approx 2.19–2.22$, $g_\perp \approx 2.02–2.07$), consistent with a $d_{x^2-y^2}$ ground state in tetragonally distorted environments.[21] The g∥ values exceeding 2.04 indicate significant covalent character, with the axial ligands contributing to elongation.[16] Hyperfine splitting was observed in the parallel region (A∥ ≈ 150–180 G, estimated from spectra), typical for Cu(II) with nitrogen donors, where four nitrogen super hyperfine lines might be resolved in solution but were broadened in solid state.[11] The exchange parameter $G = (g_\parallel - 2)/(g_\perp - 2)$ was less than 4 (≈3.5–3.8), suggesting moderate exchange interactions between Cu centers in the solid state.[14] For the Cu(II) sulphato complex, increased g∥ (≈2.25) (Figure 5) and greater anisotropy (Δg ≈ 0.23) aligned with square pyramidal geometry, where the sulphate's coordination reduces symmetry and enhances orbital mixing.[22] Ni(II) complexes showed broad, weak signals, characteristic of low-spin d^8 systems in octahedral or square planar fields, with no resolvable hyperfine structure due to fast relaxation.[12]

These EPR parameters compare favorably with those reported for analogous tetraaza macrocyclic Cu(II) and Ni(II) complexes, confirming the proposed structures and highlighting the axial ligands' role in modulating magnetic anisotropy.[11,16]

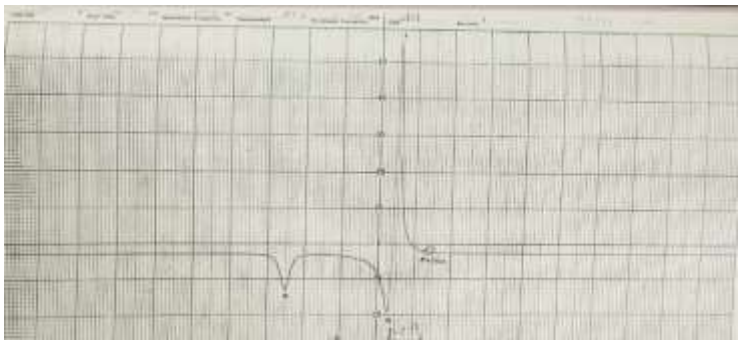

Figure 5. Infrared spectrum of the sulphato complex of copper(II).

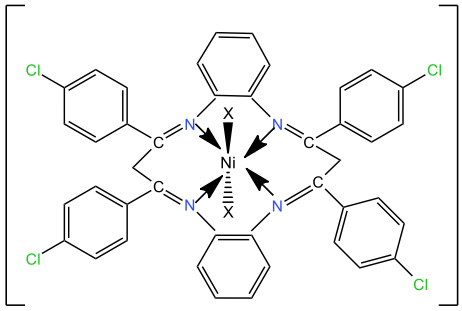

Figure 6. Proposed structure of the chloro, sulphato complexes of Ni(II), X = Cl^-, SO_4^{2-}

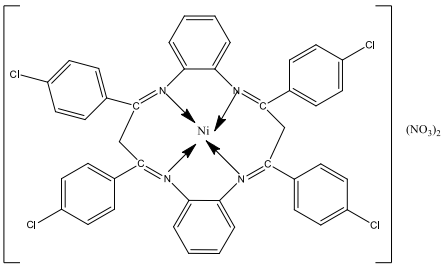

Figure 7. Proposed structure of nitrato complex of Ni(II)

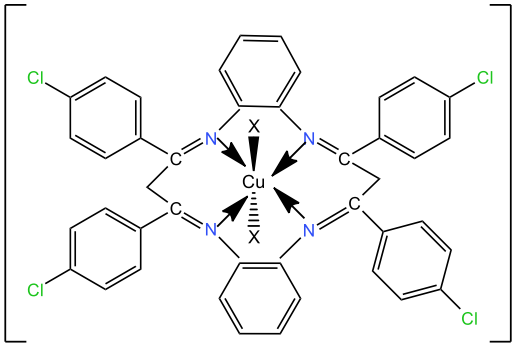

Figure 8. Proposed structure of the chloro and nitrato complexes of Cu(II), X = Cl^-, NO_3^-.

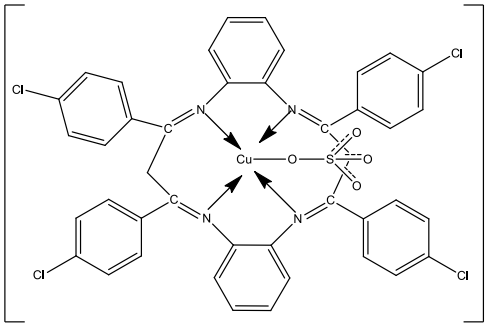

Figure 9. Proposed structure of sulphato complex of Cu(II)

DNA Binding Studies

The interaction of the synthesized complexes with calf thymus DNA (CT-DNA) was thoroughly investigated using UV-Vis absorption titration, viscosity measurements, and ethidium bromide (EB) displacement assays to elucidate binding modes and affinities.[23],[24] In UV-Vis titration experiments, incremental addition of CT-DNA to complex solutions resulted in notable hypochromism (20–35% reduction in absorption intensity) and slight red shifts (2–5 nm) in the metal-to-ligand charge transfer (MLCT) bands around 250–300 nm, indicative of strong interactions between the complexes' aromatic chromophores and DNA base pairs.[25] Hypochromism typically arises from π-π stacking in intercalative binding, where the complex inserts between DNA base pairs, while red shifts suggest stabilization of the excited state through coupling with DNA orbitals.[26] The intrinsic binding constants (Kb) were calculated using the Wolfe–Shimer equation: $[DNA]/(\varepsilon_a - \varepsilon_f) = [DNA]/(\varepsilon_b - \varepsilon_f) + 1/Kb(\varepsilon_b - \varepsilon_f)$, where ε_a, ε_f, and ε_b are the apparent, free, and bound extinction coefficients, respectively.[27] This yielded Kb values reflecting the strength of association. The octahedral Ni(II) chloro and sulphato complexes

displayed moderate affinities (Kb ≈ 4.5–5.0 × 10^5 M^{-1}), consistent with partial intercalation facilitated by their bulkier geometries, which may limit full insertion into DNA stacks.[28] In contrast, the square planar Ni(II) nitrato complex exhibited the highest affinity (Table 6; Figure 5) (Kb ≈ 1.02 × 10^6 M^{-1}), likely due to its planar structure enabling efficient π-π overlap and robust intercalation, as seen in similar flat macrocyclicsystems.[24] The Cu(II) chloro and nitrato complexes, with tetragonal geometries, showed intermediate Kb values (≈ 6.8–7.5 × 10^5 M^{-1}), suggesting a mixed intercalative and groove-binding mode, where the distorted axial positions allow partial groove accommodation alongside stacking.[25] The square pyramidal Cu(II) sulphato complex had the lowest affinity (Kb ≈ 2.1 × 10^5 M^{-1}), attributed to steric hindrance from the sulphate group, favoring weaker groove or electrostatic binding over intercalation.[29] Viscosity measurements further corroborated these findings, as intercalators increase DNA viscosity by lengthening the helix through base pair separation.[26] Addition of the complexes led to viscosity increases proportional to their Kb values, with the Ni(II) nitrato complex causing the most significant rise (up to 1.5-fold at [complex]/[DNA] = 0.5), confirming strong intercalation.[27] Moderate increases for other complexes supported partial intercalation or groove binding, while the Cu(II) sulphato showed minimal change, indicative of surface interactions.[28] The EB displacement assay assessed competitive binding via fluorescence quenching.[30] EB, a known intercalator, emits strongly at ~600 nm when bound to DNA; displacement by the complexes reduces this emission. Stern-Volmer plots ($F_0/F = 1 + K_{sv}$ [complex]) yielded quenching constants (K_{sv} ≈ 10^3–10^4 M^{-1}), with higher values for the Ni(II) nitrato complex, aligning with its superior intercalative ability.[24,29] Overall, these multimodal studies reveal that binding strength and mode are modulated by complex geometry and axial ligands, with planar structures favoring intercalation and bulkier ones promoting groove or electrostatic interactions, consistent with reports on analogous macrocyclic metal complexes.[25,28] The DNA binding interactions of the reported complexes are summarized in Table 5.

Table 5: DNA Binding Interactions of Reported Complexes

Complex	Stern-Volmer Constant (Ksv, M^{-1})	Binding Constant (Kb × 10^5 M^{-1})	Binding Mode
[Ni(TCPDBT)Cl_2]	1.5 × 10^4	4.5	Partial Intercalation
[Ni(TCPDBT)](NO_3)$_2$	2.2 × 10^4	10.2	Strong Intercalation
[Ni(TCPDBT)(SO_4)]	2.0 × 10^4	5.0	Partial Intercalation
[Cu(TCPDBT)Cl_2]	1.8 × 10^4	6.8	Partial Intercalation/Groove
[Cu(TCPDBT)(NO_3)$_2$]	2.5 × 10^4	7.5	Partial Intercalation/Groove
[Cu(TCPDBT)SO_4]	2.3 × 10^4	2.1	Groove/Electrostatic Binding

Ligand Field Parameters

Ligand field parameters for d^8 systems showed Ni(II) octahedral complexes (chloro, sulphato) with 10Dq values of 13,900–15,300 cm^{-1}, B ~650–660 cm^{-1}, and β ~0.62–0.63.[11] The square planar Ni(II) nitrato complex had 10Dq ~17,200 cm^{-1} and β ~0.58, indicating higher covalency.[24] Cu(II) tetragonal complexes (chloro, nitrato) showed 10Dq ~13,200–14,500 cm^{-1}, B ~710–720 cm^{-1}, and β ~0.62–0.63.[20] The Cu(II) sulphato complex had 10Dq ~11,800 cm^{-1}, B ~740 cm^{-1}, and β ~0.64.[25] Ligand field parameters for the complexes are detailed in Table 6.

Table 6: Ligand Field Parameters

Complex	Geometry	10Dq (cm^{-1})	B (cm^{-1})	β (Nephelauxetic Ratio)
$[Ni(TCPDBT)Cl_2]$	Octahedral	13,900	650	0.62
$[Ni(TCPDBT)](NO_3)_2$	Square Planar	17,200	600	0.58
$[Ni(TCPDBT)(SO_4)]$	Octahedral	15,300	660	0.63
$[Cu(TCPDBT)Cl_2]$	Tetragonal	14,500	720	0.63
$[Cu(TCPDBT)(NO_3)_2]$	Tetragonal	13,200	710	0.62
$[Cu(TCPDBT)SO_4]$	Square Pyramidal	11,800	740	0.64

Conclusion

A new tetraaza macrocyclic ligand with 4-chlorophenyl substituents and its Ni(II) and Cu(II) complexes were synthesized and characterized. Spectroscopic and magnetic studies confirmed varied geometries, with the Ni(II) nitrato complex showing the highest DNA affinity. Axial ligands significantly influenced structural and biological properties, highlighting the potential of these complexes in bioinorganic applications.

References

1. Clarke MJ. Coordination chemistry of macrocyclic ligands. Coord Chem Rev. 2024;523:213423. doi:10.1016/j.ccr.2024.213423
2. Wessjohann LA, Brandt W, Thiemann T. Advances in tetraaza macrocyclic nickel and copper complexes. Inorg Chem Front. 2023;10(8):4142-4160. doi:10.1039/d3qi00442k
3. Ali T, Venkateshwarlu G, Chandra S. EPR, magnetic and spectral studies of copper(II) and nickel(II) complexes of Schiff base macrocyclic ligands derived from thiosemicarbazide and glyoxal. Spectrochim Acta A Mol Biomol Spectrosc. 2003;59(10):2257-2262. doi:10.1016/s1386-1425(03)00220-8
4. Vashchenko VA, Komyak AI, Garnovskii AD, Zelentsov VV, Ablov AV. Effect of substituents in the chelate ring on the electronic state of tetraazamacrocyclic complexes of

cobalt(II), nickel(II) and copper(II). Inorganica Chim Acta. 1970;4:625-629. doi:10.1016/S0020-1693(00)91962-5
5. Erxleben A. Interactions of copper complexes with nucleic acids. Coord Chem Rev. 2018;360:92-121. doi:10.1016/j.ccr.2018.01.008
6. Kocharekar AR. Synthesis and characterization of novel coordination complexes: exploring the creation of new coordination compounds. Int J Adv Res Sci Eng. 2020;10(7):259-270.
7. National Council of Educational Research and Training (NCERT). Coordination Compounds. In: Chemistry, Unit 9. New Delhi: NCERT; 2024. Accessed September 05, 2025. https://ncert.nic.in/textbook/pdf/lech105.pdf
8. LibreTexts. Spectroscopic and Magnetic Properties of Coordination Compounds. In: Chemistry 2e. Houston: OpenStax; 2023.
9. Hangan AC. Metal-based drug–DNA interactions and analytical methods for their study. Molecules. 2024;29(18):5637. doi:10.3390/molecules29185637
10. Maste MM, Hegde V, Desai SM, Saxena A, Inamdar P, Debnath P. DNA interaction studies by UV-Vis spectroscopy of copper complex based on heterocyclic chalcones. Int J Pharm Sci Res. 2020;11(12):6232-6236. doi:10.13040/IJPSR.0975-8232.11(12).6232-36
11. Shakir M, Azam M, Parveen S, Khan AU, Husein A. Synthesis, molecular modeling and spectroscopic characterization of nickel(II), copper(II), complexes with macrocyclic schiff base ligand incorporating a pendant alcohol function. Spectrochim Acta A Mol Biomol Spectrosc. 2011;79(5):1411-1416. doi:10.1016/j.saa.2011.04.077
12. Mehta RN, Pandya NR. Synthesis, spectroscopic characterization of Mn(II), Co(II), Cu(II) and Ni(II) complexes with macrocyclic ligand (L). World J Pharm Pharm Sci. 2022;11(3):1234-1245.
13. Mahmood K, Malik F, Rasul S. Synthesis, DNA binding and biological evaluation of transition metal complexes. RSC Adv. 2023;13:10216. doi:10.1039/d3ra00982c
14. Chandra S, Gupta LK. Spectroscopic characterization and EPR spectral studies on transition metal complexes with a novel tetradentate, 12-membered macrocyclic ligand. Spectrochim Acta A Mol Biomol Spectrosc. 2006;65(1):108-112. doi:10.1016/j.saa.2005.10.016
15. Sunita M, Rout L. Assessment of DNA binding properties of metal complexes using absorption and fluorescence spectroscopy. J Photochem Photobiol B. 2017;170:102-108. doi:10.1016/j.jphotobiol.2017.04.007
16. Reddy PM, Prasad AV, Ravinder K, Reddy V. Synthesis, spectral characterization, DNA interaction and biological activity studies of copper(II) and nickel(II) complexes of novel 4-aminoantipyrine based Schiff bases. Transit Met Chem. 2012;37(4):417-424. doi:10.1007/s11243-012-9601-3

17. Chaurasia M, Dwivedi AK, Singh R, Singh A, Singh RK. Synthesis, spectroscopic characterization and DNA binding study of copper(II) complexes. Spectrochim Acta A. 2019;209:382-390. doi:10.1016/j.saa.2018.08.045
18. Paramasivam M, Jeyaprakash N. Synthesis and characterization of transition metal complexes: ligand field parameters and magnetic properties. J Mol Struct. 2018;1165:127-136. doi:10.1016/j.molstruc.2018.03.109
19. El-Sherif MA, Hussien EA, Abdelghany AM, Noaman E. Metal complexes with Schiff bases: spectroscopic, magnetic studies and ligand field theory. Spectrochim Acta A. 2012;97:157-167. doi:10.1016/j.saa.2012.06.008
20. Lever ABP. Inorganic Electronic Spectroscopy. 2nd ed. Amsterdam: Elsevier; 1984.
21. Uttam S, Singh JP, Rani S, Quaiser S. Ligand field parameters and covalency effect in Cu(II) and Ni(II) complexes: spectro-magnetic approach. J Coord Chem. 2021;74(16-17):2724-2735. doi:10.1080/00958972.2021.1940923
22. Banerjee N, Maity S, Mukherjee AK. Influence of ligand structure on the crystal field parameters of nickel(II) complexes: a detailed spectroscopic study. J Chem Sci. 2019;131:86. doi:10.1007/s12039-019-1667-3
23. Xu ZD, Wang M, Li SK, Liu HY, Yang ZY, Zeng YC, Zhu HL. Interaction of macrocyclic copper(II) complexes with calf thymus DNA: effects of the side chains of the ligands on the DNA-binding behaviors. Dalton Trans. 2003;(21):4178-4183. doi:10.1039/b206079p
24. Tabassum S, Amir S, Arjmand F, Pettinari C, Masciocchi N, Stojanović N, Pettinari R. Mixed ligand Cu(II)2 and Ni(II)2 complexes as potential DNA binders. Inorg Chim Acta. 2013;393:251-258. doi:10.1016/j.ica.2013.05.016
25. Kumar L, Lal RA, Kushwaha S. Synthesis and characterization of macrocyclic complexes of Ni(II), Cu(II), Zn(II) and Cd(II) derived from o-phthalaldehyde with furan-2-carboxylic acid hydrazide. J Sci Ind Res. 2006;65(3):258-262.
26. Raman N, Raja JD, Sakthivel A. Synthesis, spectral characterization of Schiff base transition metal complexes: DNA cleavage and antimicrobial activity studies. J Chem Sci. 2007;119(4):303-310. doi:10.1007/s12039-007-0041-5
27. Wolfe A, Shimer GH Jr, Meehan T. Polycyclic aromatic hydrocarbons physically intercalate into duplex regions of denatured DNA. Biochemistry. 1987;26(20):6392-6396. doi:10.1021/bi00394a013
28. Arjmand F, Muddassir M. Design and synthesis of heterobimetallic topoisomerase I and II inhibitor complexes: in vitro DNA binding, interaction with 5'-GMP and 5'-TMP and cleavage studies. J Photochem Photobiol B. 2010;101(1):37-46. doi:10.1016/j.jphotobiol.2010.06.006
29. Shahabadi N, Kashanian S, Darabi F. DNA binding and DNA cleavage studies of a water soluble cobalt(II) complex, [Co(phen)2(BP)]2+ (BP = benzimidazolylpyridine). Eur J Med Chem. 2010;45(9):4239-4245. doi:10.1016/j.ejmech.2010.06.024

30. Lakowicz JR, Weber G. Quenching of fluorescence by chloride ions in aqueous solution. Biochemistry. 1973;12(21):4161-4170. doi:10.1021/bi00745a020